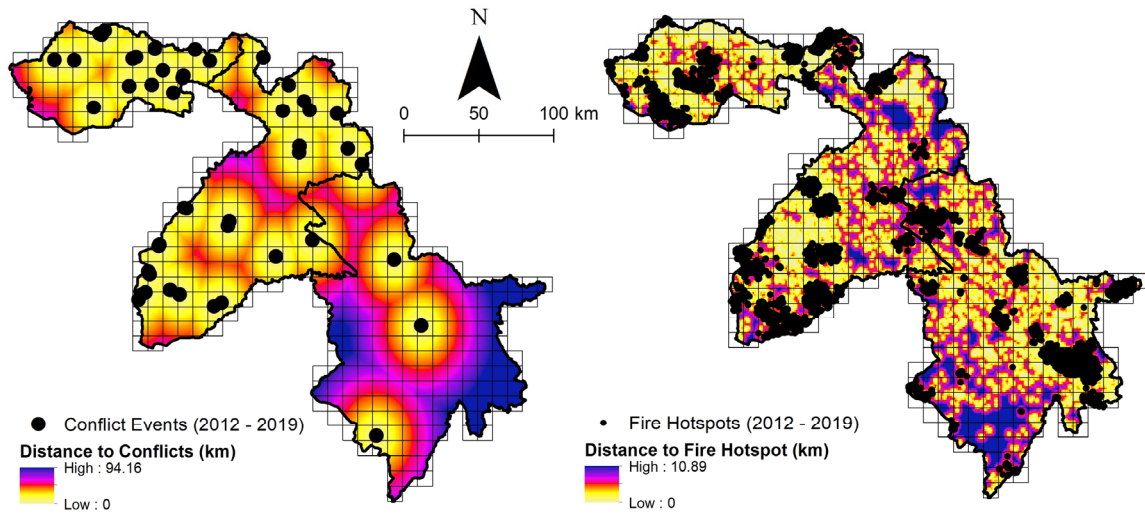
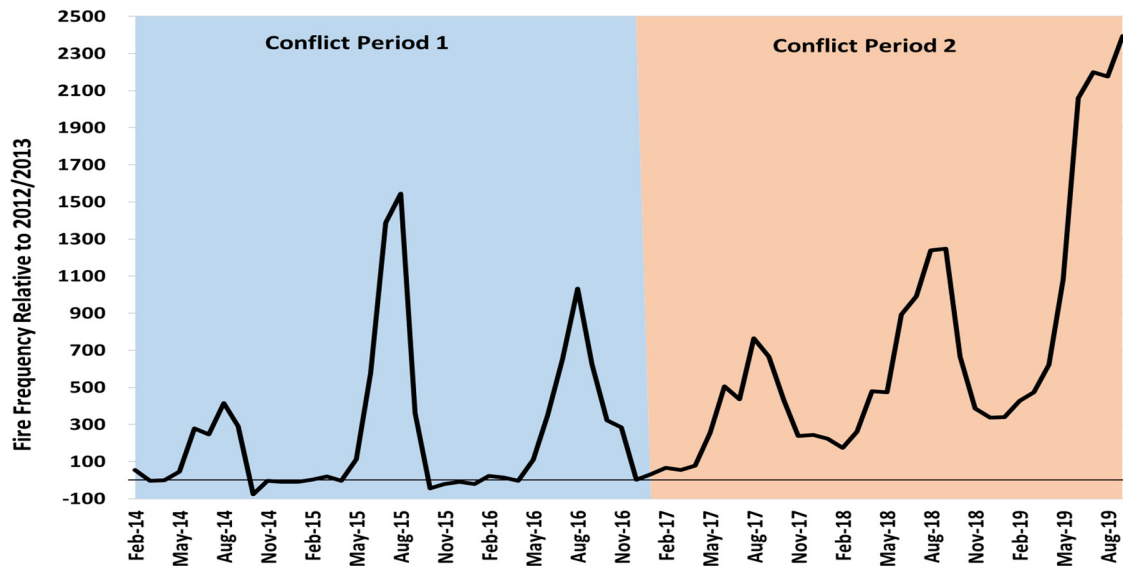


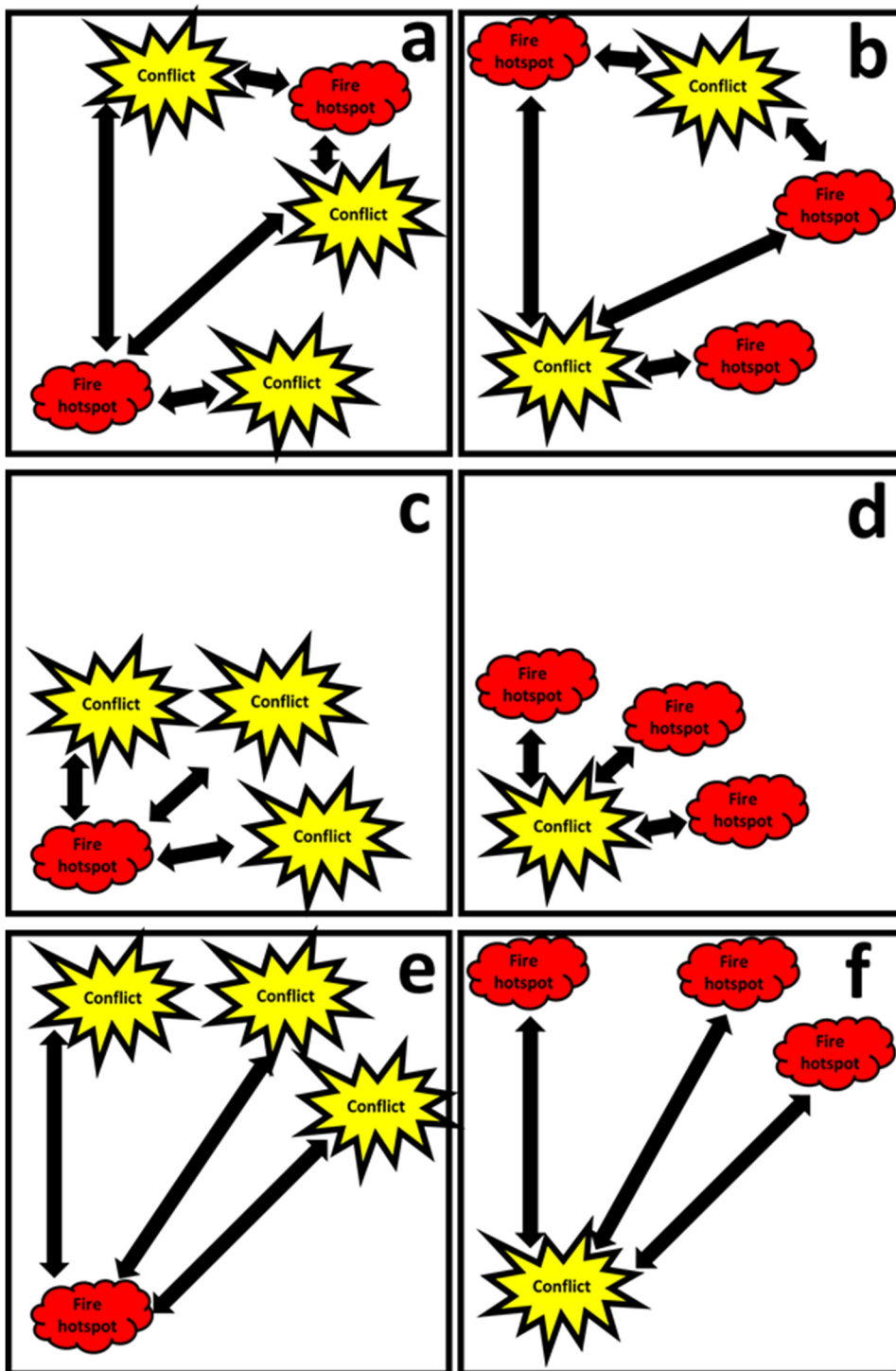
Supplementary Information



Supplementary Figure S1. Distance metrics included in the partial correlation analysis. The conflict events are the raw untransformed data, from which Euclidean distances were calculated on a gridded surface. The fire hotspots are clusters derived from Getis-Ord G_i^* analysis (see methods). The fishnet is spaced at 10 km intervals.

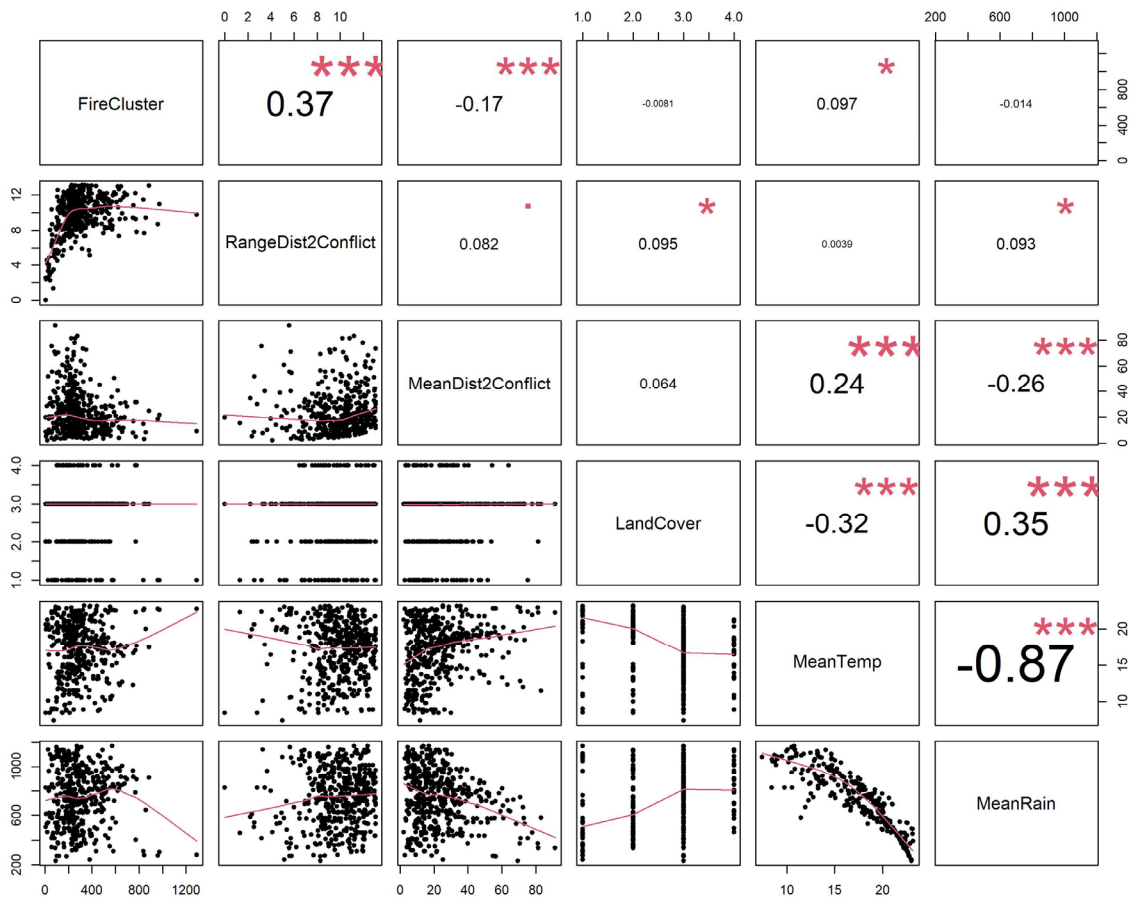


Supplementary Figure S2. Temporal fire anomalies relative to 2012 and 2013 when the prevalence of conflict was low. The anomalous peak in the summer of 2015 corresponds to the 29 conflicts and 5504 fire events that occurred in the region. The large peak in 2019 corresponds to intensification of the Turkish offensive in the KR-I.

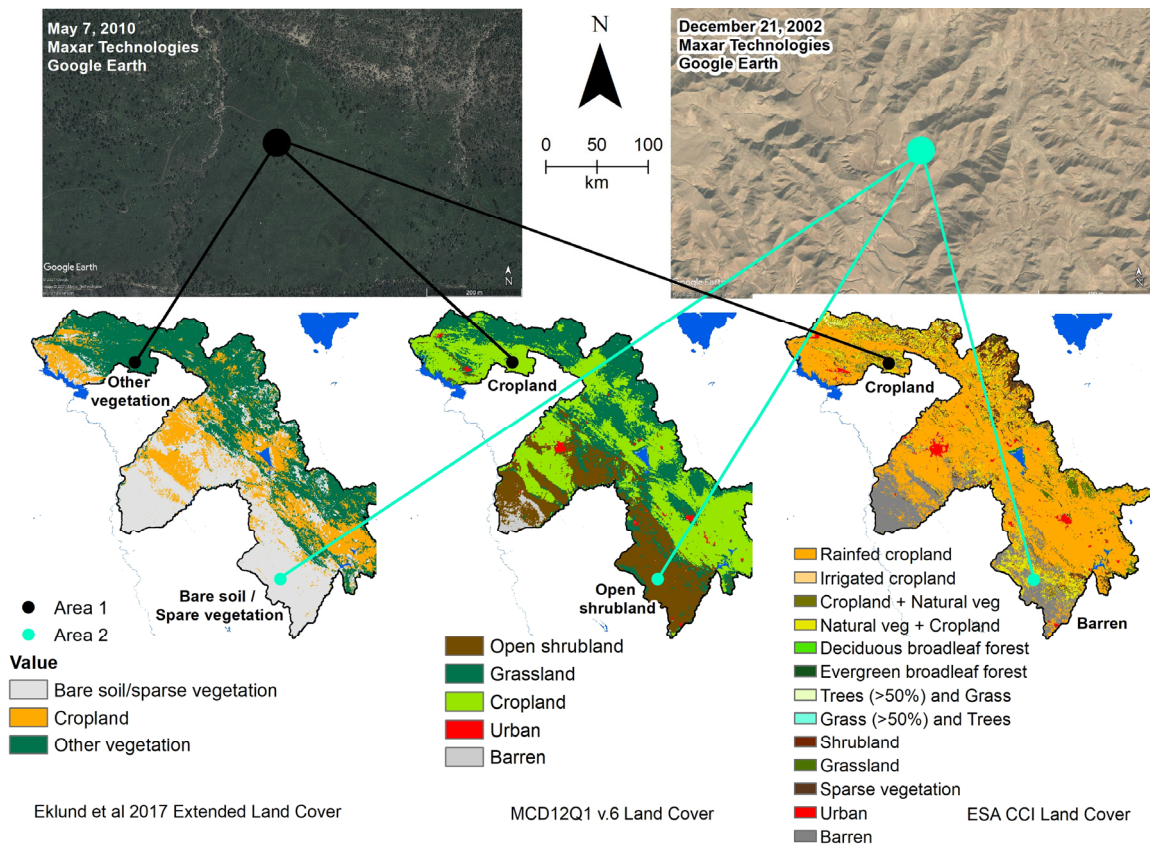


Supplementary Figure S3. Visual representation of different scenarios in the relationship between the amplitude of the distance fire hotspots and conflict events within a 10 km x 10 km fishnet cell. Panel a and b have the highest amplitude, i.e. the largest range of distances to conflict, while panels c – f have low amplitudes despite the fact that c and d have a shorter overall distances to conflict while e and f have longer overall distances. The amplitude is the difference between the shortest and longest distance to conflict. In the correlation analysis, a and b would have a high positive correlation whereas c through f would have a negative correlation as distance to conflict. Because the dependent

variable is the sum of the fire radiative power clusters within each cell, it seems to be more favorable for fire to have more variability in distances to conflict therein.



Supplementary Figure S4. Scatterplot matrix of the conflict, fire, land cover, and climatic variables within the fishnet cells. *RangeDist2Conflict* is the amplitude of the Euclidean distances from each conflict location; *FireCluster* is the hotspot analysis that was produced using the Getis-Ord G_i^* approach (see methods); *LandCover* is the variability of land cover classes within each 10 km fishnet cell; *MeanTemp* and *MeanRain* are mean annual temperature and mean annual rainfall between 2000 and 2019. The red stars indicate the level of statistical significance (*** = $P < 0.0001$, ** = $P < 0.001$, * = $P < 0.01$, · = $P < 0.05$).



Supplementary Figure S5.: Comparison between the land cover dataset used in this study (250 m) versus the MODIS MCD12Q1 land cover product (500 m, version 6) and the ESA CCI Land Cover product (300 m, version 2.1.1). The other vegetation class was created specifically to avoid mischaracterization of certain vegetation areas in rugged topographies that contain a mixture of land cover classes. Similarly, other land cover categories, such as the bare soil/sparse vegetation are able to reasonably capture those areas compared to the MCD12Q1 product. Similarly, the ESA CCI product does not fare better in the northern mountainous areas where it considerably overestimates croplands.